Appl. sci. Res. Section A, Vol. 11

THE EFFECT OF A STANDING SOUND FIELD ON A SLOW STREAM DISCHARGED FROM A POROUS WALL

by J. KESTIN*) and L. N. PERSEN**)

Summary

The paper discusses the flow pattern which results when a stationary sound field is created outside an infinite plane wall through which a fluid is slowly discharged. It is shown that the field can be obtained as a simple superposition of the secondary flow field calculated by H. Schlichting and the velocity of discharge. Flow patterns are sketched and one of them is compared with a photograph obtained by R. M. Fand and J. Kaye under sufficiently similar conditions. The agreement between the two patterns is very satisfactory.

§ 1. *Introduction.* In an experimental study of the effect of sound on natural convection from horizontal cylinders, Fand and Kaye[1]) examined visually the resulting flow field by discharging smoke from a row of hypodermic needles in an arrangement sketched in fig. 1. In the absence of the sound field, the hypodermic needles supplied vertical, evenly spaced threads of smoke. However, when a standing acoustic wave (i.e. two plane waves s_1 and s_2 in fig. 1 propagating in opposite directions) was superimposed, it was noticed that the threads of smoke showed a marked tendency to move away from the velocity loops and to crowd towards the pressure loops (velocity nodes), figs. 2 and 3. This rather curious flow pattern induced by the sound field can be easily explained by the appearance of secondary flow (acoustic streaming) near the plane of discharge.

*) Professor of Engineering, Brown University, Providence, R.I.

**) Professor of Mechanics, Norges Tekniske Høgskole, Trondheim, Norway; Visiting Professor at Brown University.

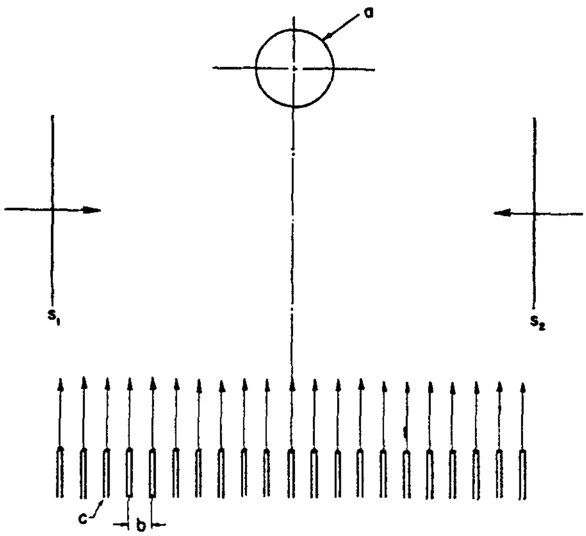

Fig. 1. Arrangement used by R. M. Fand and J. Kaye[1]).
a. Experimental tube
b. Separation between hypodermic needles (*8* inch)
c. Row of hypodermic needles discharging smoke
s_1, s_2. Two plane waves resulting in a standing wave.

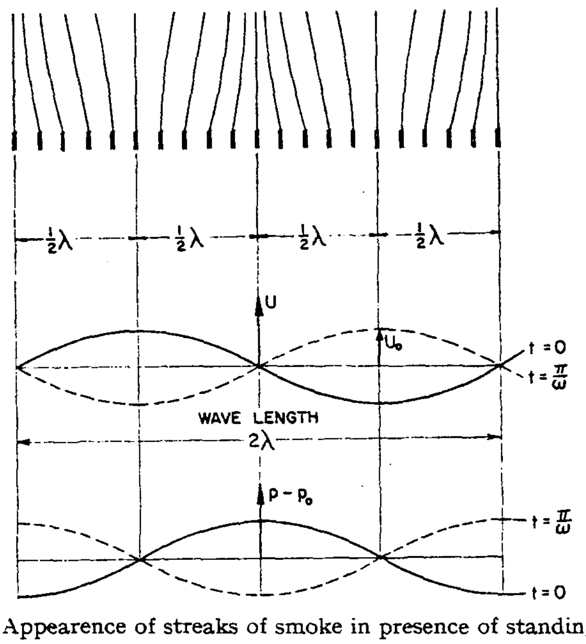

Fig. 2. Appearence of streaks of smoke in presence of standing wave.

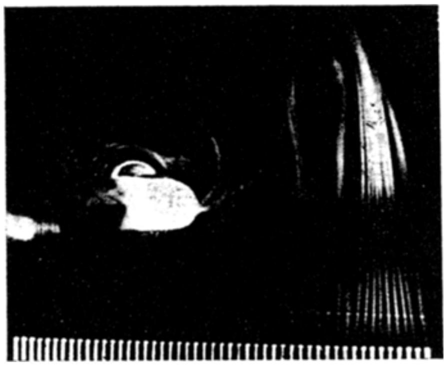

Fig. 3. Appearance of streaks as photographed by R. M. Fand and J. Kaye[1] in presence of standing wave.

Wavelength	$2\lambda = 16.4$ cm
Frequency	$f = 2130$ cps
	$(\omega = 2\pi f = 13{,}390\ \text{sec}^{-1})$
Distance between nozzles	$b = \frac{1}{8}$ inch
Discharge velocity	$v_0 = 30$ cm/sec (rough estimate)

(Courtesy Dr. R. M. Fand)

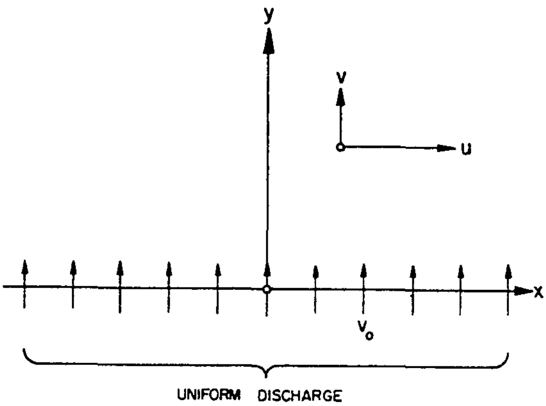

Fig. 4. The idealized problem.

In order to demonstrate that this is the case, we shall examine the flow pattern which exists on one side of an infinite plane, fig. 4, through which an incompressible fluid is discharged uniformly at a velocity v_0 in the y-direction. The sound field creates a flow field at a large distance from the wall whose component parallel to the wall is described by

$$U(x, t) = U_0 \sin(\pi x/\lambda) \cos(\omega t), \tag{1}$$

where λ is the half-wavelength, and $\omega = 2\pi f$ is the circular frequency of the acoustic oscillation. The velocity amplitude

$$U_1(x) = U_0 \sin(\pi x/\lambda) \tag{2}$$

is here a function of the co-ordinate along the wall, as shown in the lower graph of fig. 2. As is well-known, a good approximation to the pressure field is given by

$$\frac{\partial}{\partial x} [p(x, t)] = -\rho \frac{\partial U}{\partial t},$$

or by

$$p(x, t) - p_0 = -(\rho\omega\lambda U_0/\pi) \cos(\pi x/\lambda) \sin(\omega t), \tag{3}$$

the pressure nodes coinciding with the velocity loops and *vice versa*.

§ 2. *Formulation and solution of the problem.* The problem as stated can be solved by the application of the iterative scheme used by Schlichting to determine the flow field about an oscillating cylinder[2][3]) and by the assumption that the velocity of discharge v_0 merely constitutes a boundary condition for the component v of velocity at $y = 0$. This is the assumption usually made in the theory of suction or discharge through a boundary layer[3]). This assumption implies that the momentum of the fluid being discharged can be neglected, and that its velocity of discharge is, therefore, small compared with a representative velocity in the oscillating stream, say its maximum value U_0, so that

$$v_0 \ll U_0. \tag{4}$$

Thus the problem is governed by the boundary layer equations

$$\begin{gathered}\frac{\partial u}{\partial x} + \frac{\partial v}{\partial y} = 0, \\ \frac{\partial u}{\partial t} + u\frac{\partial u}{\partial x} + v\frac{\partial u}{\partial y} = -\frac{1}{\rho}\frac{\partial p}{\partial x} + \nu\frac{\partial^2 u}{\partial y^2}, \\ -\frac{1}{\rho}\frac{\partial p}{\partial x} = \frac{\partial U}{\partial t} + U\frac{\partial U}{\partial x},\end{gathered} \tag{5}$$

subject to the boundary conditions

$$\begin{aligned} u &= 0,\ v = v_0 \quad \text{at} \quad y = 0, \\ u &= U(x, t) \quad\ \ \text{at} \quad y = \infty. \end{aligned} \tag{5a}$$

So formulated, the problem is identical with the one solved by Schlichting[2][3] the analogy extending even to equation (2) which describes the velocity amplitude. Indeed, for an infinite cylinder

$$U_1(x) = 2U_0' \sin(x/R) \cos(\omega t), \tag{2a}$$

with the radius R playing the same part as $1/\pi$'th part of half the wavelength in our problem, and the velocity amplitude U_0' being equal to $\frac{1}{2}U_0$ in (2). The only difference consists in the fact that now $v = v_0$ at $y = 0$, whereas in Schlichting's problem it was stipulated that $v = 0$ at $y = 0$.

It is not difficult to guess that the secondary flow pattern in the present case will be obtained by the superposition of the uniform, parallel velocity v_0 upon the streaming pattern obtained by Schlichting. This fact can be ascertained by retracing the steps of the derivation. Since an adequate derivation is easily accessible[2], we shall do this in a somewhat sketchy fashion.

The complete flow pattern consists of the series

$$\begin{aligned} u(x, y, t) &= u_1(x, y, t) + u_2(x, y, t) + \dots, \\ v(x, y, t) &= v_1(x, y, t) + v_2(x, y, t) + \dots. \end{aligned} \tag{6}$$

of which only two terms are computed. The first terms satisfy the linear equations

$$\begin{aligned} \frac{\partial u_1}{\partial t} - \nu \frac{\partial^2 u_1}{\partial y^2} &= \frac{\partial U}{\partial t}, \\ \frac{\partial u_1}{\partial x} + \frac{\partial v_1}{\partial y} &= 0, \end{aligned} \tag{7}$$

with the boundary conditions

$$\begin{aligned} u_1 &= 0,\ v_1 = v_0 \quad \text{at} \quad y = 0, \\ u_1 &= U(x, t) \quad\ \ \text{at} \quad y = \infty. \end{aligned} \tag{7a}$$

This being a linear problem with linear boundary conditions, it is sufficient to copy Schlichting's solution adding v_0 to his v_1. Thus

$$\begin{aligned} u_1 &= U_1(x)[f_1(\eta) \sin(\omega t) + f_2(\eta) \cos(\omega t)], \\ v_1 &= v_0 - (\nu/2\omega)^{\frac{1}{2}} \frac{dU_1}{dx} [g_1(\eta) \sin(\omega t) + g_2(\eta) \cos(\omega t)], \end{aligned} \tag{8}$$

with

$$\begin{aligned}
f_1(\eta) &= -\exp(-\eta)\sin\eta, \\
f_2(\eta) &= 1 - \exp(-\eta)\cos\eta, \\
g_1(\eta) &= \exp(-\eta)(\sin\eta + \cos\eta) - 1, \\
g_2(\eta) &= 2\eta - 1 - \exp(-\eta)(\sin\eta - \cos\eta),
\end{aligned}$$

and

$$\eta = y(\omega/2\nu)^{\frac{1}{2}}. \tag{8b}$$

The velocity components u_1 and v_1 contribute only the term v_0 to streaming, as the time-averages of all the remaining terms vanish. In Schlichting's problem there was no contribution at all, and the terms u_1 and v_1 were required for the computation of the convective terms in the differential equations for the second terms, u_2 and v_2. These are obtained from the equations

$$\begin{gathered}
\frac{\partial u_2}{\partial t} - \nu\frac{\partial^2 u_2}{\partial y^2} = U\frac{\partial U}{\partial x} - u_1\frac{\partial u_1}{\partial x} - v_1\frac{\partial u_1}{\partial y}, \\
\frac{\partial u_2}{\partial x} + \frac{\partial v_2}{\partial y} = 0,
\end{gathered} \tag{9}$$

with the boundary conditions

$$\begin{aligned}
&u_2 = 0 \text{ and } v_2 = 0 \quad \text{at} \quad y = 0, \\
&u_2 = 0 \qquad\qquad\qquad \text{at} \quad y = \infty,
\end{aligned} \tag{9a}$$

which are identical with Schlichting's. It is easy to see that the right-hand side of the first equation (9) will consist of terms multiplying $\sin\omega t$, $\cos\omega t$, $\sin 2\omega t$, $\cos 2\omega t$ and a free term. The free term is a function of x and y and arises from $\sin^2\omega t$, $\cos^2\omega t$. On collecting terms, it is found that this free term determines the portion of u_2 and v_2 which does not vanish on averaging. The only remaining problem is to ascertain whether the appearance of v_0 in the second equation (8) contributes to this term. This can be immediately answered in the negative, since v_0 will appear multiplying $\sin\omega t$ and $\cos\omega t$. In this manner we have satisfied ourselves that Schlichting's expressions for u_2 and v_2 solve the present problem also, due regard being paid to the introduction of the changes ennumerated in connection with (2a).

The flow field will thus be described by the averaged components

$$\begin{aligned} \bar{u} &= -\frac{U_1}{2\omega}\frac{\mathrm{d}U_1}{\mathrm{d}x}h'(\eta), \\ \bar{v} &= v_0 + \frac{1}{\omega}\left(\frac{\nu}{2\omega}\right)^{\frac{1}{2}}\frac{\mathrm{d}}{\mathrm{d}x}\left[U_1\frac{\mathrm{d}U_1}{\mathrm{d}x}\right]h(\eta), \end{aligned} \tag{10}$$

with

$$\begin{aligned} h'(\eta) &= \tfrac{3}{2} - \eta\exp(-\eta)(\sin\eta - \cos\eta) - \\ &\quad - \exp(-\eta)(\cos\eta + 4\sin\eta) - \tfrac{1}{2}\exp(-2\eta), \\ h(\eta) &= \tfrac{3}{2}\eta + \eta\exp(-\eta)\sin\eta - \tfrac{1}{4}[1 - \exp(-2\eta)] + \\ &\quad + \exp(-\eta)(2\sin\eta + 3\cos\eta) - 3. \end{aligned}$$

The flow pattern consists, as stated, of a superposition of the uniform field v_0 on the one calculated by H. Schlichting.

The streaming pattern in a two-dimensional Kundt tube was calculated by Lord Rayleigh[4][5]. It is essentially the same as the above, and the effect of a slow discharge upon it can also be computed by superposition*).

The preceding formulae, as shown in detail in [2]) are restricted to small oscillations. More precisely they are valid on condition that

$$\frac{U\partial U/\partial x}{\partial U/\partial t} \ll 1.$$

Introducing the estimates

$$\partial U/\partial t \sim \omega U_0;\quad U\partial U/\partial x \sim \pi U_0^2/\lambda,$$

and noting that $\omega\lambda/\pi = a$, we obtain the restriction

$$\frac{U_0}{a}\frac{\cos^2(\omega t)\cos(\pi x/\lambda)}{\sin(\omega t)} \ll 1.$$

Here we may put $\cos(\pi x/\lambda) = 1$, but the functions of time may not

*) Equations (37) and (38) on p. 339 in ref. 4 contain a misprint, and should read

$$\left.\begin{aligned} u_2 = -\frac{u_0^2\sin(2kx)}{8a}\Big\{&\exp(-\beta y)[4\sin\beta y + 2\cos\beta y + \exp(-y)] + \\ &+ \frac{3}{2} - \frac{9}{2}\frac{(y_1-y)^2}{y_1^2} + \frac{21}{4\beta y_1^3}(y_1-y)^2 - \frac{21}{4\beta y_1}\Big\}. \end{aligned}\right\}\ \text{Lord Rayleigh (37)}$$

$$\left.\begin{aligned} v_2 = -\frac{2ku_0^2\cos(2kx)}{8\beta a}\Big\{&\exp(-\beta y)[\sin\beta y + 3\cos\beta y + \tfrac{1}{2}\exp(-\beta y)] + \\ &+ \frac{3}{2}\beta(y_1-y) - \frac{3}{2}\beta\frac{(y_1-y)^3}{y_1^2} + \frac{7}{4y_1^3}(y_1-y)^3 - \frac{21}{4y_1}(y_1-y)\Big\}. \end{aligned}\right\}\ \text{Lord Rayleigh (38)}$$

be replaced by their maximum values since $\sin(\omega t)$ vanishes when $\cos^2(\omega t) = 1$. Rather, it is necessary to examine the function

$$\varphi(t) = \cos^2(\omega t)/\sin(\omega t), \tag{11}$$

shown plotted in fig. 5. The graph reveals that $U_0\varphi/a$ remains extremely small under most conditions, since normally

$$U_0/a \ll 1. \tag{12}$$

Even with $\varphi = 10$, condition (12) will be satisfied for $U_0/a = 0.01$ over 15/16th of a period, the criterion $U_0\varphi/a$ having a value of only 0.1.

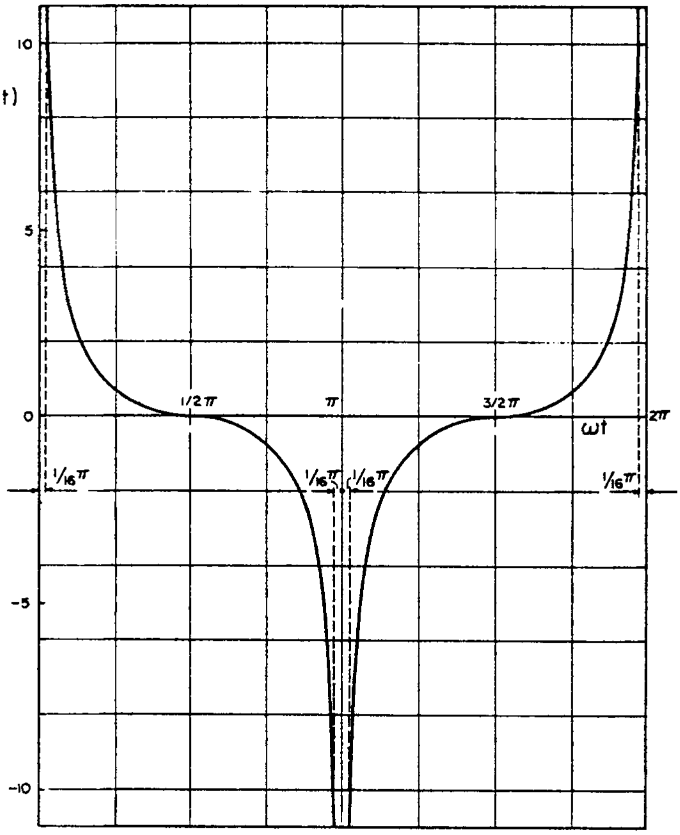

Fig. 5. Plot of $\varphi(t)$ from eq. (11).

In addition to the restrictions (12) and (4), it is necessary to realize that the assumption of an incompressible fluid makes it impossible for the solution (10) to be valid far away from the wall·

§ 3. *Flow patterns.* The velocity field whose components were given in eq. (10) can also be described by the stream function

$$\psi = -v_0 x - \frac{U_1}{\omega}\frac{\mathrm{d}U_1}{\mathrm{d}x}\left(\frac{\nu}{2\omega}\right)^{\frac{1}{2}} h(\eta) \tag{13}$$

where $h(\eta)$ was given in eq. (10a). Substituting U_1 from eq. (2), it is possible to give it the dimensionless form

$$\frac{a}{U_0}\{\psi/\tfrac{1}{2}U_0\delta_{ac}\} = -[Ka\cdot\xi + \sin(2\pi\xi)\cdot h(\eta)], \tag{14}$$

where

$$Ka = 4\frac{\lambda}{\delta_{ac}}\frac{a}{U_0}\frac{v_0}{U_0}. \tag{14a}$$

Here $a = \omega\lambda/\pi$ is the velocity of sound, and

$$\delta_{ac} = (2\nu/\omega)^{\frac{1}{2}} \tag{14b}$$

is the *ac* boundary layer thickness, also known as the depth of penetration. The problem has been expressed in terms of the ratios

$$\eta = y/\delta_{ac} \tag{14c}$$

and

$$\xi = x/\lambda \tag{14d}$$

as the independent variables. It should be noted that ξ varies from 0 to 1 over one half wavelength, and that even at short distances from the plate η will be very large since δ_{ac} can be exceedingly small. The problem contains a single dimensionless parameter Ka, which we propose to call the Kaye number; it characterizes the relation between the velocity of discharge v_0 and the sound field, and depends on three ratios whose physical significance can be easily identified (after the late Joseph Kaye).

In order to gain an insight into the appearance of the flow field, it is instructive to examine the flow patterns shown in figures 6 to 9. The diagram in fig. 6 shows the pattern of streamlines for $Ka = 0$, that is in the absence of blowing. Figure 7 contains auxiliary plots of the two components of streaming from (10). It is noted that the $\bar{v}$-component passes through zero at a distance δ_v' which separates the lower closed vortex from the upper loop. The value of δ_v'

is determined by the condition that $h(\eta) = 0$, (10*a*). A graphical solution of this equation gives

$$\delta_v' = 1.88\delta_{ac}, \tag{15}$$

approximately, with δ_{ac} from (14*b*). The $\bar{v}$-component passes through a maximum at a distance δ_v'' at which the $\bar{u}$-component vanishes. This distance is determined by the condition that $h'(\eta) =$ $= 0$, (10*a*), and it is found that

$$\delta_v'' = 1.18\delta_{ac}. \tag{15a}$$

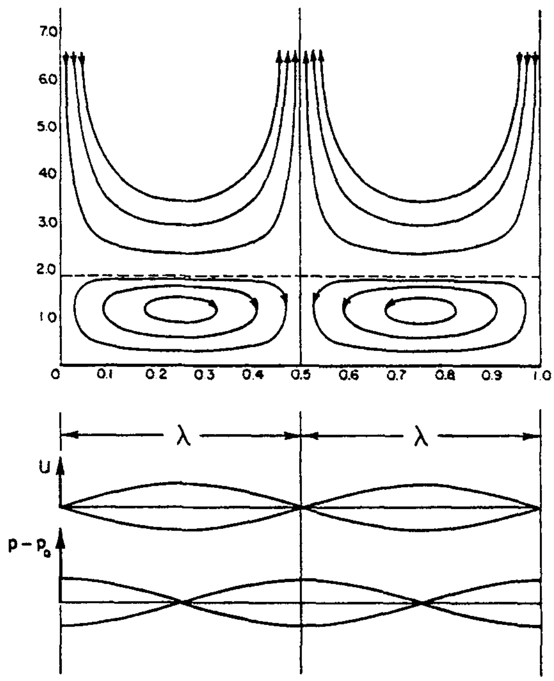

Fig. 6. Flow pattern in absence of blowing ($Ka = 0$).

The two maxima in the $\bar{u}$-component occur at

$$\delta_u' = 4.37\delta_{ac}, \tag{15b}$$

and

$$\delta_u'' = 0.55\delta_{ac}, \tag{15c}$$

respectively. In view of the extreme smallness of δ_{ac}, all these distances turn out to be very small, it being noted that they are all independent of the x-co-ordinate.

The asymptotic value for the $\bar{u}$-component is

$$\bar{u}_\infty = -\frac{3}{8}\frac{U_0^2}{a}\sin(2\pi x/\lambda). \tag{16}$$

The two maxima in $\bar{u}$ have the values

$$\overline{u'_{\max}} = 1.05\bar{u}_\infty, \tag{16a}$$

and

$$\overline{u''_{\max}} = -0.17\bar{u}_\infty, \tag{16b}$$

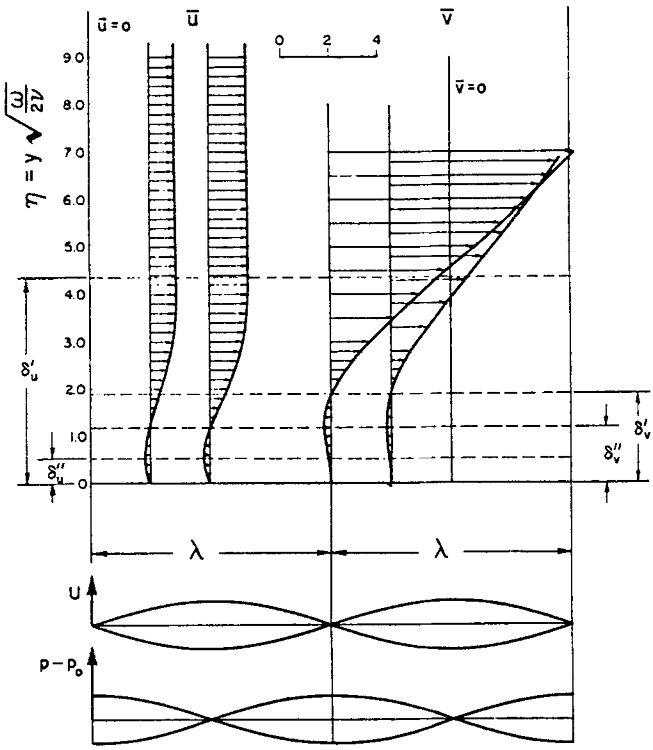

Fig. 7. Velocity profiles in absence of blowing ($Ka = 0$).

respectively; they are small compared with U_0 since U_0/a is usually small. The maximum in $\bar{v}$ has a value

$$\overline{v_{\max}} = 0.32\frac{U_0^2}{a}\frac{\delta_{ac}}{\lambda}\cos(2\pi x/\lambda), \tag{16c}$$

which is exceedingly small.

When a uniform velocity v_0 is superimposed on the preceding pattern, the flow will first be deflected towards the velocity loops corresponding to the negative values of $\bar{u}$ below δ_v''. The direction

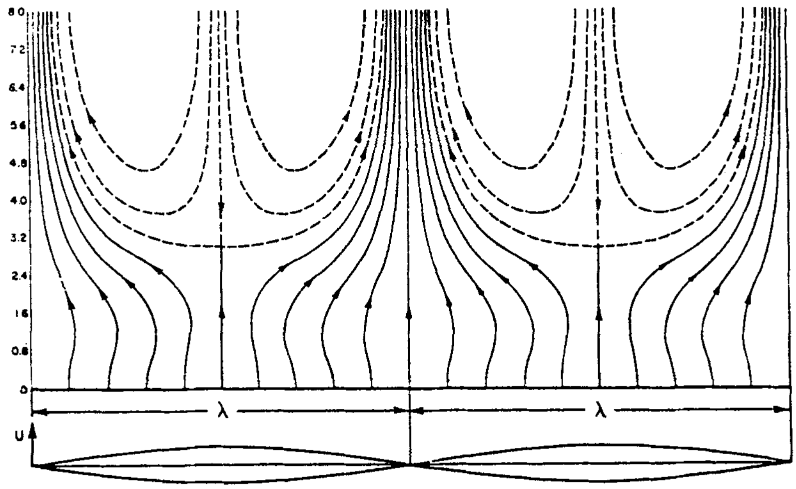

Fig. 8*a*. Effect of blowing on secondary flow in the presence of a stationary sound field, $Ka = 1$.

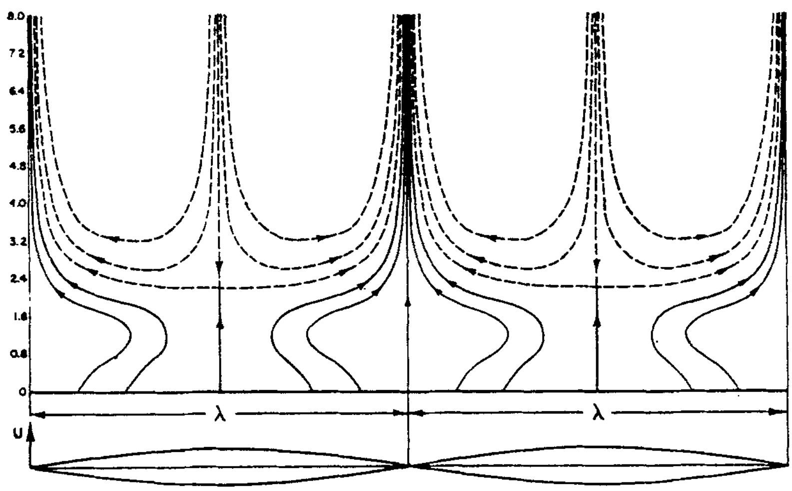

Fig. 8*b*. Effect of blowing on secondary flow in the presence of a stationary sound field, $Ka = 2$.

of the slope will change towards the velocity nodes at larger distances owing to the change in the direction of $\bar{u}$, the extreme smallness of the distance δ_v'' will suppress the former, and only the latter slopes will be discernible to the eye in a smoke pattern.

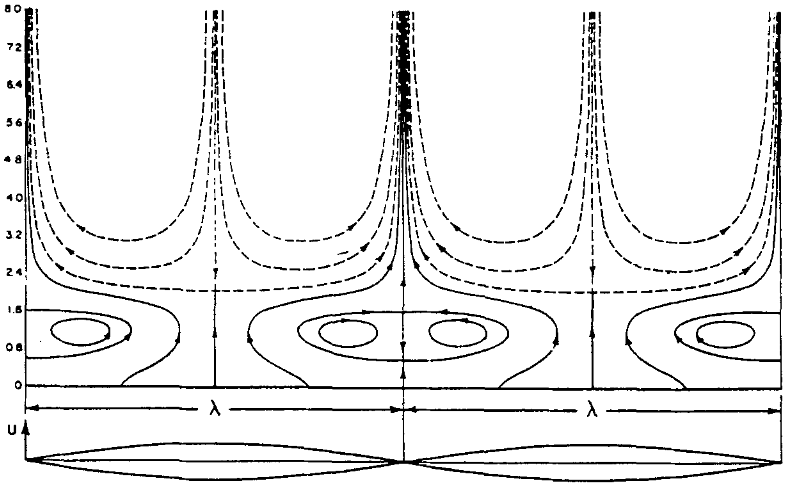

Fig. 8*c*. Effect of blowing on secondary flow in the presence of a stationary sound field. $Ka = 10$.

The change in the flow pattern caused by blowing is shown in fig. 8 for the Kaye number assuming the values of 1, 2 and 10. These values correspond to low frequencies (relatively large δ_{ac}) or extremely low velocities of discharge, v_0. The diagrams show clearly that the streamlines first move away from the velocity nodes but crowd towards them higher above the plate. They also illustrate the fact that even very slow blowing deeply affects the pattern of streamlines which turns out to be extremely sensitive.

The final diagram, fig. 9, represents the flow pattern for the conditions under which Fand and Kaye obtained the photograph in fig. 3. Utilizing the data given in the caption, we can compute the following values. It is recalled that the sound pressure level, L_p, is defined as

$$L_p = 20 \log(\Delta p/\Delta p_0),$$

with $\Delta p_0 = 2 \times 10^{-5}$ Newton/m². Here Δp denotes the rms pressure amplitude, i.e.

$$\Delta p = (p - p_0)/\sqrt{2}.$$

Making use of (3) it is easy to derive that

$$U_0 = \Delta_{p_0} \, 10^{L_p/20} \, \sqrt{2}/(\rho a),$$

with $\rho = 1.29$ kg/m^3 and $a = 350$ m/sec, it is found that

$$U_0 = 2.1 \text{ m/sec.}$$

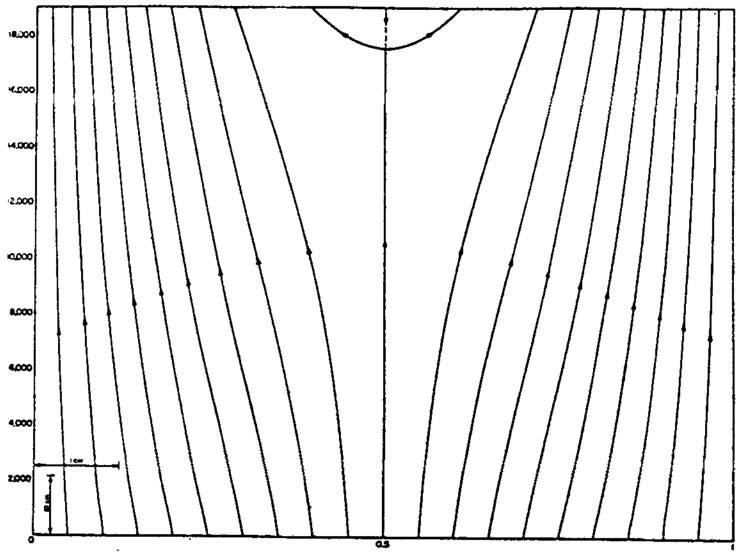

Fig. 9 Flow pattern calculated for the conditions under which R. M. Fand and J. Kaye obtained the photograph in fig. 3. $Ka = 166 \times 10^3$.

Furthermore, employing the value $\nu = 0.15$ cm^2/sec, we can calculate that

$$\delta_{ac} = 0.47 \times 10^{-2} \text{ cm},$$

which is extremely small compared with the scale of the photograph. Noting that $\lambda = a/2f$, we find

$$\lambda = 8.2 \text{ cm},$$

which agrees with the distance between the loops as measured with respect to the spacing ($\frac{1}{8}$ inch) of the hypodermic needles.

Substituting these values into (12*a*), it is found that

$$Ka = 166 \times 10^3,$$

which is very large owing to the high frequency and the smallness of δ_{ac}. Under these conditions, only the pattern above δ_v can be sketched. The agreement between the calculated and observed flow patterns is quite striking.

Acknowledgements. The authors wish to thank Drs. M. G. Scherberg and R. M. Fand for drawing their attention to the present problem and Dr. R. M. Fand for generously supplying them with a print for fig. 3 and with all the data pertaining to it. The work was performed with the financial assistance of the Aeronautical Research Laboratory of the Office of Scientific Research, U.S. Air Force (Contract AF 33(616)-7749) and of the National Science Foundation (Grant G-16158). Mr. B. C. Shen, Research Assistant at Brown University performed all calculations and prepared the drawings.

Received 5th October, 1961.

REFERENCES

1) Fand, R. M. and J. Kaye, Trans. ASME **83** (J. Heat Transf.) (1961) 133.
2) Schlichting, H., transl. J. Kesting, Boundary Layer Theory, 4th. ed., McGraw-Hill, 1960, p. 224.
3) Schlichting, H., Physikalische Zeitschrift **33** (1932) 327.
4) Lord Rayleigh, The Theory of Sound, vii, p. 337, Dover Publ., 1945.
5) Lord Rayleigh, Phil. Trans. **175** (1883) 1.